

## Field-induced antiferromagnetism and competition in the metamagnetic state of terbium gallium garnet

K. Kamazawa,<sup>1</sup> Despina Louca,<sup>1,\*</sup> R. Morinaga,<sup>2</sup> T. J. Sato,<sup>2</sup> Q. Huang,<sup>3</sup> J. R. D. Copley,<sup>3</sup> and Y. Qiu<sup>3,4</sup>

<sup>1</sup>*Department of Physics, University of Virginia, Charlottesville, Virginia 22904, USA*

<sup>2</sup>*Neutron Science Laboratory, Institute for Solid State Physics, University of Tokyo, 5-1-5 Kashiwanoha, Kashiwa, Chiba 277-8581, Japan*

<sup>3</sup>*NIST Center for Neutron Research, Gaithersburg, Maryland 20899, USA*

<sup>4</sup>*Dept. of Materials Science and Engineering, University of Maryland, College Park, Maryland, 20742, USA*

(Received 2 June 2008; published 13 August 2008)

The magnetic properties of the hyperkagome system of  $\text{Tb}_3\text{Ga}_5\text{O}_{12}$  have been investigated by neutron scattering. Evidence of antiferromagnetic long-range order of the Tb moments at  $T_N \leq 0.35$  K in zero field is provided. With the application of magnetic field in the paramagnetic phase, ferromagnetic peaks initially appear at nuclear Bragg reflections. With the field higher than 3 Tesla, antiferromagnetic Bragg peaks appear as well indicating that the low-temperature magnetic phase extends well beyond the phase boundary, into the paramagnetic phase, with field. The new magnetic symmetry sets in at the metamagnetic transition in this system.

DOI: 10.1103/PhysRevB.78.064412

PACS number(s): 75.30.Kz, 61.05.F-, 75.50.Ee

When physical systems have access to more than one ground state, collective effects invoked from the competition or frustration of the interactions may emerge leading to exotic phases.<sup>1</sup> Even in crystals with pristine order, the presence of residual entropy at low temperatures is evidence of frustration inherent to the lattice.<sup>2</sup> In a typical crystal, atoms along with their magnetic moments, if present, are expected to follow certain symmetry rules. In magnetism, the Curie-Weiss,  $\theta_{CW}$ , temperature<sup>3</sup> defines an approximate scale at which point long-range ordering should appear. However, magnetic spinels, pyrochlores, and garnets defy this classic notion precisely because of their crystal symmetry.<sup>4-6</sup> If spins reside at the corners of triangular or tetrahedral lattices, the pairwise spin interactions cannot be simultaneously satisfied if they are to be aligned antiferromagnetically.<sup>7</sup> Such geometric frustration gives rise to a macroscopic degenerate ground-state manifold. In quantum spin systems, exotic collective effects may give rise to a resonating valence bond state.<sup>8</sup> In classical spin systems, frustration may lead to a spin-liquid state where the spins fluctuate continuously down to absolute zero,<sup>9</sup> or to a spin-ice state as in the paradigmatic hexagonal ice.<sup>10,11</sup>

In the rare-earth (RE) garnets with  $Ia\bar{3}d$  symmetry, the classical RE spin resides at the corners of triangles organized in two interpenetrating sublattices forming a hyperkagome structure<sup>1</sup> as seen in Fig. 1(a). In some garnets such as the  $\text{Gd}_3\text{Ga}_5\text{O}_{12}$  with a Heisenberg spin, magnetic long-range order is suppressed all the way down to  $\sim 0$  K.<sup>12,13</sup> However, in garnets of the Tb family such as  $\text{Tb}_3\text{Al}_5\text{O}_{12}$ , the paramagnetic (PM) state makes way to static antiferromagnetic (AF) order.<sup>14</sup> Intriguing is the Ising-like nature of the Tb spin with local axes that point in three orthogonal directions in the triangle,<sup>15</sup> producing a multiaxis magnet with potentially different responses to external perturbations such as an applied magnetic field.<sup>14</sup> The low-energy physics is dominated by two crystal-field ground-state singlets of this non-Kramers ion, while magnetic interactions which mixes them give rise to Néel order in the absence of an external magnetic

field.<sup>16,17</sup> Thus, long-range dipolar interactions and nearest-neighbor exchange interactions play an important role in determining the magnetic properties, and the competition and balance between the two may yield either an ordered or a frustrated state<sup>2</sup> of which this system is susceptible to given the geometry of the Tb lattice. For this we have studied  $\text{Tb}_3\text{Ga}_5\text{O}_{12}$  (TGG) which has no reported transition thus far.<sup>18</sup>

Using elastic neutron scattering, an AF magnetic transition is observed for the first time at  $T_N \leq 0.35$  K, which is much lower than the Curie-Weiss temperature,  $\Theta_{CW} \sim 8.61$  K. Using inelastic neutron scattering, a single-ion anisotropy excitation is observed in the PM phase with a characteristic energy of 0.2 meV that splits to two singlet peaks at  $\sim 0.15$  and 0.3 meV upon cooling due to interspin interactions.<sup>19</sup> Additionally, a field-induced transition is observed at temperatures above  $T_N$ . Previous studies on other garnet systems focused on the field effects of the Néel state and little is known of the field effects in the PM state. Our results on TGG show that the AF phase extends well beyond the AF-PM phase boundary with field. With the magnetic field turned on, the excitations due to single-ion crystal field transitions are quickly suppressed as they are replaced by static magnetic correlations. Initially ferromagnetic peaks appear at nuclear reflections with no nuclear intensity due to polarization of the PM phase. At  $H > 3$  T, the neutron results show the appearance of the same AF Bragg peaks observed below  $T_N$  and with no field, indicating the onset of a magnetically ordered phase. The ordered moment is below the local free Tb ion value ( $9.72 \mu_B$ ) that in turn suggests that exchange interactions are still important. It is interesting to note that the field at which this occurs corresponds to the field at which the first metamagnetic transition is observed in TGG.<sup>20</sup> Metamagnetic transitions are ubiquitous, appearing not only in garnets<sup>21</sup> but in other systems as well.<sup>22</sup> In TGG, the first magnetization plateau appears at magnetic fields,  $H > 3$  T, followed by a second step at  $H > 10$  T of which transitions become increasingly sharper with cooling. It has

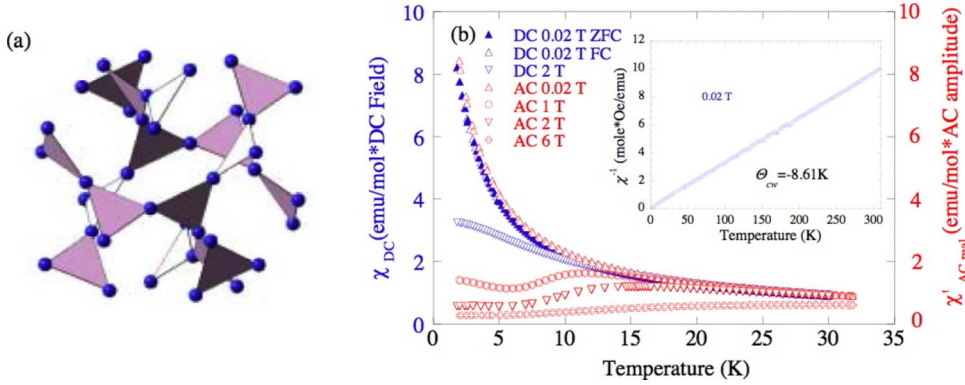


FIG. 1. (Color online) (a) The Tb triangular sublattice in the garnet structure is shown. In (b), the dc and ac magnetic susceptibility,  $\chi_{DC}(T)$  (blue) and  $\chi'_{AC}(T)$  (red) are shown. At 0.02 T, the ZFC and FC data of  $\chi_{DC}(T)$  overlap indicating no spin-glass phase. With increasing field, deviations from Curie-Weiss law are observed. The inset is a plot of  $1/\chi$  as a function of temperature at  $H = 0.02$  T.

been suggested that low-lying crystal field level crossing can explain the metamagnetic transition but this may not be the only contributing factor.<sup>20</sup> The magnetic structure is reproduced by breaking the  $Ia\bar{3}d$  symmetry at the  $a$  glide and most likely contributes to the stability of the metamagnetic transition. The new symmetry allows both ferromagnetic and antiferromagnetic interactions within the triangle that in turn may be a source of competition and frustration.

A powder sample of single phase Tb<sub>3</sub>Ga<sub>5</sub>O<sub>12</sub> with the cubic  $Ia\bar{3}d$  crystal symmetry was prepared by standard solid-state reaction method. Elastic and inelastic neutron measurements were performed at the BT-1 diffractometer using a Ge (311) monochromator of the NIST Center for Neutron Research (NCNR) using a 7 T vertical magnet and at the DCS spectrometer using an 11.5 T vertical magnet with a dilution refrigerator and incident wavelengths of 2.5 and 7 Å. The refinement of the magnetic structures was done using the GSAS package.<sup>23</sup> Although  $|\theta_{CW}|$  is estimated to be about 8.61 K [shown in inset of Fig. 1(b)], no magnetic transition is evident at this temperature. Zero-field-cooled (ZFC) and field-cooled (FC) curves of the bulk susceptibility,  $\chi_{DC}(T)$ , at small applied fields are identical [Fig. 1(b)], and the real part of  $\chi'_{AC}(T)$  shows almost no frequency dependence (not shown in the figure).  $\chi'_{AC}(T)$  follows a typical paramagnetic behavior where the rise can be fit by a Curie-Weiss term. Thus, unlike observations of spin-glass phase in triangular kagome lattices<sup>24</sup> or spin-liquid correlations<sup>12</sup> or spin freezing<sup>13</sup> that may develop with cooling in isomorphous Gd<sub>3</sub>Ga<sub>5</sub>O<sub>12</sub>, this garnet appears to be an ordinary paramagnet. With increasing field, however, unusual paramagnetic behavior is observed. The tail end of the curve that is weakly temperature-dependent remains unaffected, but the rise at low temperatures no longer overlaps. For fields of  $H \geq 1$  T, the  $\chi_{DC}(T)$  curves deviate from simple Curie-Weiss behavior and the field response is clearly nonlinear. In  $\chi'_{AC}(T)$ , an inflection appears that shifts to higher temperatures with increasing field that is indicative of a transition. Similar measurements on pyrochlores<sup>25</sup> attributed the inflection in  $\chi'_{AC}(T)$  to single moment saturation signaling a new form of collective paramagnetic behavior.

Zero-field and field-induced transitions even in the presumed PM phase are observed in this garnet, revealing a complex phase diagram where the AF phase extends beyond the phase boundary. The momentum transfer,  $Q$ , dependence of the elastic neutron scattering intensity at  $H=0$  T shows

the appearance of new peaks at (1, 1, 0) and (3, 1, 0) below 0.35 K that are AF in nature indicating the onset of a Néel state [see Fig. 2(d)]. Although weak in intensity, these peaks are not allowed by the nuclear symmetry while the integer peak indices suggest no doubling of the magnetic unit cell. Additionally, the (2, 1, 1) Bragg peak is observed at this temperature indicating ferromagnetic (FM) correlations. This is allowed by the crystal symmetry but no nuclear intensity appears because it cancels out in the structure function. The presence of the (1, 1, 0), (3, 1, 0), and (2, 1, 1) peaks indicates the onset of static ferromagnetic, as well as antiferromagnetic, ordering of Tb spins and the emergence of an AF magnetic phase as seen in other garnets.<sup>21</sup> At temperatures above 0.35 K, when the field is turned on, intensity under several nuclear Bragg peaks, such as (2, 0, 0) and (2, 1, 1), first appears, as well as increase in intensity of the (2, 2, 0) peak, indicating that static FM coupling between Tb spins is induced [Fig. 2(c)]. By  $H \geq 4$  T, [Fig. 2(b)] the AF peaks observed in the pattern of Fig. 2(d) at 0.35 K and 0 T reappear showing for the first time a field-induced AF transition in the PM phase. This structure persists up to at least 11.5 T, the maximum field reached in our experiment. Figure 2(f) shows the Rietveld refined model at 6 T that includes both nuclear and magnetic structures. Details of the magnetic structure will be given below. In Fig. 2(g) the temperature dependence of select Bragg peaks in magnetic fields of 2 (solid line) and 6 T (dotted line). The intensity falls off with increasing temperature for all Bragg peaks shown, (2, 0, 0), (2, 1, 1), and (2, 2, 0). Note that the field-induced transition is quite sharp at 2 T, with the upturn occurring around 15 K. Thus the inflection in  $\chi'_{AC}(T)$  clearly corresponds to the onset of a polarized paramagnetic state with static ferromagnetic correlations. At  $H=6$  T, the intensity of the peaks drops off gradually and is extrapolated to approach zero around 35 K. The gradual decrease occurs over a larger temperature range in the 6 T field and this may well be due to staggered fields.<sup>26</sup> Figure 2(h) shows the integrated intensity of purely magnetic peaks, such as (1, 1, 0) and (3, 1, 0), as well as mixed magnetic and nuclear peaks, such as (2, 0, 0), (2, 2, 0), and (2, 1, 1), at  $\sim 1$  K as a function of field. The mixed (magnetic and nuclear) Bragg peak intensities rise almost immediately from a very small value and saturate beyond 2 T except for the (200) that decreases in intensity. On the other hand, the purely magnetic peaks are not discernible until about 4 T at which field the peaks are observed above background and continue to grow.

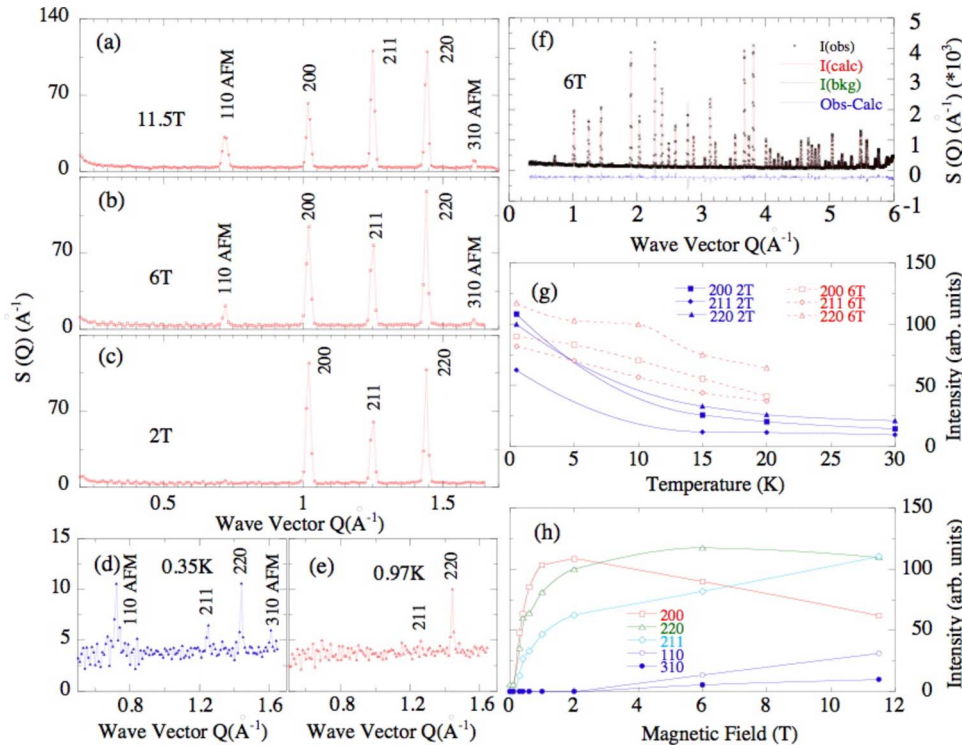


FIG. 2. (Color online) Neutron diffractograms [(a)–(f)] as a function of temperature and field. With the temperature set at  $\sim 0.5$  K, the field is changed from 11.5 T in (a), to 6 T in (b), to 2 T in (c), and to 0 T in (e). In (d), the temperature is changed to 0.35 K at 0 T. These data were collected using DCS with a wavelength of 7 Å and a full profile refinement is not reliable because of the limited number of Bragg peaks. In (f), the refined model for the 6 T data is compared to the diffraction data collected at BT-1. In (g), the temperature dependence of Bragg peaks at 2 and 6 T is shown. In (h), the field dependence of Bragg peaks is shown. Error bars represent  $\pm$  one standard deviation.

The refined magnetic configuration at two representative fields, 1 and 4 T, are summarized in Table I. With the field on, spins order in FM chains as seen in the model of Fig. 3 (left) creating a polarized PM state. The field at which the new magnetic structure first appears corresponds to the metamagnetic plateau phase. The ordered moment at 4 T averaged between refinements of BT-1 and DCS data is  $\sim 7\mu_B$ , less than the free Tb moment ( $9.72\mu_B$ ). The metamagnetic transition extends from  $\sim 3 < H < 10$  T as seen in the  $M(H)$  curve of Fig. 3 for data collected at 1.8 K. At the onset of the steplike plateau, spin canting breaks the  $a$ -glide symmetry of the  $Ia\bar{3}d$  symmetry and allows for the AF ordering of spins as shown in the model of Fig. 3 (right), which is the refined structure corresponding to fields from 4 to 11.5 T. The presence of AF and FM correlations create a canted ferrimagnetic state. We were not able to go beyond 11.5 T to investigate the second plateau. Given that the low-lying crystal-field levels crossing occurs at fields less than 1 T,<sup>27</sup> the stability of the metamagnetic transition is most likely enhanced by the long-range magnetic interactions emerging from the new symme-

try. The continuous crystal field crossing alone cannot explain the appearance of the AF peaks. For fields ranging from 4 to 11.5 T, we observed how the spin direction at the three sublattices continuously changes while maintaining the same structure. At the same time, we also observed the presence of small crystal structure distortions with field as shown in Table II, which suggests that small changes in the local dodecahedral Tb environment may subsequently affect the crystal-field bands. This additionally indicates that the ex-

TABLE I. FM and AF magnetic structures at 1 and 4 T, respectively. The Tb ion occupies the 24c site. The Tb ions are separated to three groups, red at  $(0, \pm 1/4, 1/8)$  yellow at  $(1/8, 0, \pm 1/4)$ , and blue at  $(\pm 1/4, 1/8, 0)$ . Each vector spin has two components, where one component is always positive and the second component can be positive or negative. This is the component that is indicated in the table.

	Red	Yellow	Blue
AF	+ - - - + - +	+ - - - + - +	++++ - - - -
F	++++ + + + +	++++ + + + +	++++ + + + +

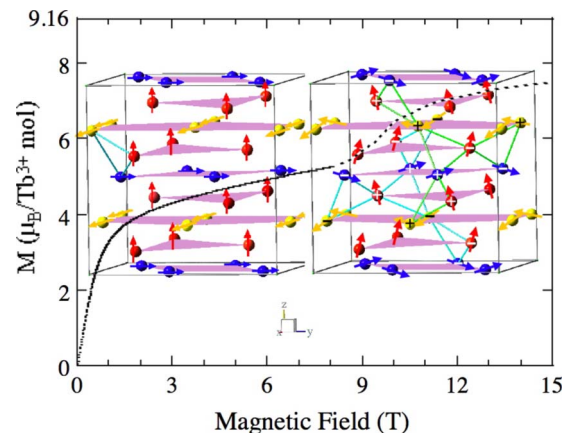


FIG. 3. (Color online) A plot of the magnetization curve as a function of field,  $M(h)$ , is shown in the background at 1.8 K. The dotted line is data obtained from Ref. 20. Two magnetic structure models are shown: the model on the left represents the structure corresponding to the rise in  $M(h)$ ; the model on the right represents the magnetic structure of the plateau state. The vectors corresponding to the Tb spins are colored red, yellow, and blue indicating the three sublattices. The + and - signs indicate the direction of the vector spin.

TABLE II. A list of Tb-O bond lengths and O-Tb-O bond angles within the dodecahedral environment of Tb as a function of field at 0.5 K. The values were obtained from the Rietveld refinement of the diffraction data from the BT-1 instrument which has high resolution. Data at higher fields were collected on the DCS instrument and the resolution is not as good. The goodness of fit,  $\chi^2$ , for the refinement is also shown. The refined ordered moment averaged over refinement of DCS and BT-1 data reached a value of  $\sim 8 \mu_B$  by 6 T.

Field	Tb-O (1) Å	Tb-O (2) Å	O-Tb-O (1)°	O-Tb-O (2)°	$\chi^2$
0	2.458	2.362	166.042	160.230	1.844
1	2.461	2.359	165.823	160.293	1.784
2	2.474	2.358	166.189	159.578	2.233
4	2.454	2.367	166.363	160.120	3.763
6	2.446	2.359	165.932	160.632	3.035

change coupling between nearest neighbors,  $J_{nn}$ , is not necessarily isotropic. The fact that both FM and AF interactions are simultaneously present may result in competition.

In addition to the static magnetic structure, we investigated the magnetic dynamics with field and temperature. The

neutron dynamic structure function,  $S(\omega)$ , shown in Fig. 4 is  $Q$  integrated from 0.5 to 1.65 Å<sup>-1</sup>. With the field off and the temperature set in the PM phase, a single broad peak appears at an energy centered around 0.2 meV [Fig. 2(a)]. This is due to the Tb single-ion anisotropy. With further cooling, the singlet peak splits to two, at  $\sim 0.15$  and 0.3 meV, with an energy difference  $\Delta \sim 0.15$  meV. The intensity of the lower energy peak increases continuously, even below  $T_N$ . The 0.3-meV peak shows almost no dispersion while the 0.15-meV peak shows dispersion. This is shown in the inset of Fig. 2(b). The minima in the dispersion coincide with the  $Q$  positions of the AF peaks in Fig. 2(d). The field dependence of the inelastic peaks is shown in Fig. 2(b). With small field values, the two singlet peaks shift to the right because of increasing the Zeeman splitting. However, at  $H=0.6$  T, a gap opens up while the two peaks merge to one. The gap appears to be of the order of 0.15 meV. For fields higher than 2 T, the peaks are either suppressed or become too weak to be detected from the background and the gap disappears.

The phase boundary between the AF and PM phases is unlike the other garnets studied thus far. The presumed PM phase is quite rich with the AF phase extending well beyond the boundary of 0.35 K. In the Néel state, the area under the lower energy inelastic peak is larger and the split can be reproduced by considering a Hamiltonian with interspin dipolar interactions using a mean-field random phase approximation.<sup>28</sup> The finite excitation gap above  $T_N$  is intriguing. Static FM correlations are present when the gap first appears while the gap closes when static AF correlations set in and the magnetic symmetry breaks. The spin arrangement within the triangle results in bonds with FM and AF interactions. Even though there are long-range dipolar interactions, competition between the FM and AF interactions may result in frustration even in the ordered state.<sup>4</sup> Our neutron results demonstrate for the first time how a frustrated state may be induced with a magnetic field and how the magnetic symmetry breaking is necessary for the stability of the metamagnetic transition in this garnet.

The authors would like to acknowledge valuable discussions with B. Gaulin, Y. B. Kim, S.-H. Lee, and S. Poulton for help with the BT-1 experiment. Work at the University of Virginia is supported by the U. S. Department of Energy, under Contract No. DE-FG02-01ER45927. The use of the Neutron Scattering facilities at NIST was supported in part through NSF Grant No. DMR-0454672 .

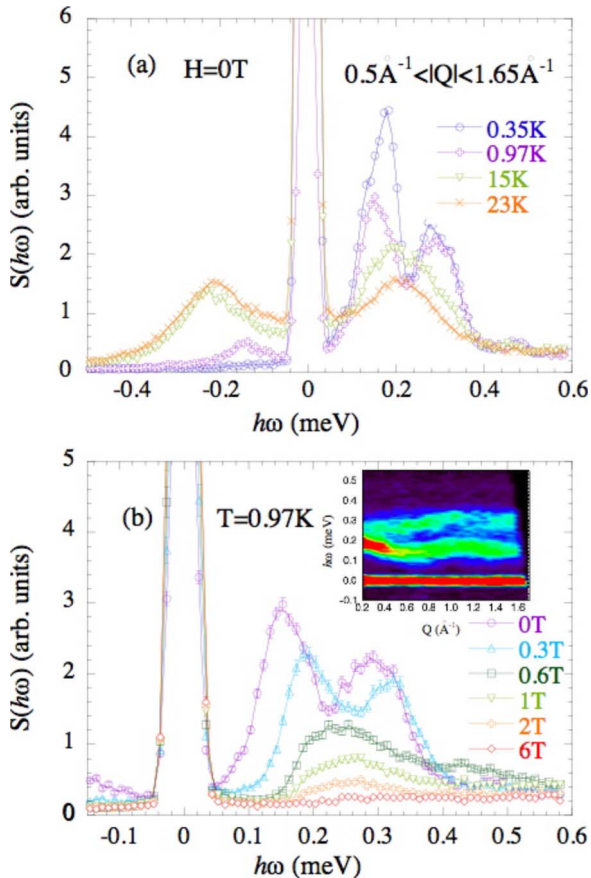


FIG. 4. (Color online) (a) A plot of the temperature dependence of  $S(\omega)$  as a function of energy. A single peak is evident at high temperatures that splits to two with cooling. The two singlets persist even in the Néel phase. The lower energy peak becomes more populated with cooling. (b) A plot of the field dependence of  $S(\omega)$  at  $\sim 1$  K. With increasing field, the two singlets gradually shift to higher energies while their intensity decreases. At 0.6 T, they merge to one peak while their intensity is suppressed even further and fade into the background above 2 T. The inset shows the  $Q$  dependence of the two modes.

\*louca@virginia.edu

- <sup>1</sup>A. P. Ramirez, in *Handbook on Magnetic Materials*, edited by K. J. H. Busch (Elsevier, Amsterdam, 2001), Vol. 13, p. 423.
- <sup>2</sup>T. Yoshioka, A. Koga, and N. Kawakami, *J. Phys. Soc. Jpn.* **73**, 1805 (2004).
- <sup>3</sup>A. Morrish, *The Physical Principles of Magnetism* (Wiley, New York, 1965).
- <sup>4</sup>S. T. Bramwell and M. J. O. Gingras, *Science* **294**, 1495 (2001).
- <sup>5</sup>S.-H. Lee, C. Broholm, W. Ratcliff, G. Gasparovic, Q. Huang, T. H. Kim, and S. W. Cheong, *Nature (London)* **418**, 856 (2002).
- <sup>6</sup>M. J. Harris, S. T. Bramwell, D. F. McMorrow, T. Zeiske, and K. W. Godfrey, *Phys. Rev. Lett.* **79**, 2554 (1997).
- <sup>7</sup>I. Mirebeau, I. N. Goncharenko, P. Cadavez-Pares, S. T. Bramwell, M. J. P. Gingras, and J. S. Gardner, *Nature (London)* **420**, 54 (2002).
- <sup>8</sup>P. W. Anderson, *Phys. Rev.* **102**, 1008 (1956).
- <sup>9</sup>R. Moessner and J. T. Chalker, *Phys. Rev. Lett.* **80**, 2929 (1998).
- <sup>10</sup>L. Pauling, *J. Am. Chem. Soc.* **57**, 2680 (1935).
- <sup>11</sup>J. Snyder, J. S. Slusky, R. J. Cava, and P. Schiffer, *Nature (London)* **413**, 48 (2001).
- <sup>12</sup>O. A. Petrenko, C. Ritter, M. Yethiraj, and D. McK Paul, *Phys. Rev. Lett.* **80**, 4570 (1998).
- <sup>13</sup>P. Schiffer, A. P. Ramirez, D. A. Huse, P. L. Gammel, U. Yaron, D. J. Bishop, and A. J. Valentino, *Phys. Rev. Lett.* **74**, 2379 (1995).
- <sup>14</sup>B. E. Keen, D. P. Landau, and W. P. Wolf, *Phys. Lett.* **23**, 202 (1966).
- <sup>15</sup>J. Felsteiner and S. K. Misra, *Phys. Rev. B* **24**, 2627 (1981).
- <sup>16</sup>R. Bidaux, A. Gavignet-Tillard, and J. Hammann, *J. Phys. (Paris)* **34**, 19 (1973).
- <sup>17</sup>J. Hammann, *Acta Crystallogr., Sect. B: Struct. Crystallogr. Cryst. Chem.* **25**, 1853 (1969).
- <sup>18</sup>The measurements by A. H. Cooke, T. L. Thorp, and M. R. Wells, *Proc. Phys. Soc. London* **92**, 400 (1967) only went down to 0.6 K.
- <sup>19</sup>R. J. Birgenau, *Magnetism and Magnetic Materials-1972*, AIP Conf. Proc. No. 10, edited by C. D. Graham and J. J. Rhyne (AIP, New York, 1973), Pt. 2, p. 1664.
- <sup>20</sup>M. Guillot, A. Marchand, V. Nekvasil, and F. Tcheou, *J. Phys. C* **18**, 3547 (1985).
- <sup>21</sup>B. E. Keen, D. Landau, B. Schneide, and W. P. Wolf, *J. Appl. Phys.* **37**, 1120 (1966).
- <sup>22</sup>H. Kobayashi and T. Haseda, *J. Phys. Soc. Jpn.* **19**, 765 (1964).
- <sup>23</sup>GSAS, A. Larson and R. B. Von Dreele, Los Alamos National Laboratory Report No. LAUR-86-748, 1986 (unpublished).
- <sup>24</sup>A. P. Ramirez, G. P. Espinosa, and A. S. Cooper, *Phys. Rev. Lett.* **64**, 2070 (1990).
- <sup>25</sup>B. G. Ueland, G. C. Lau, R. J. Cava, J. R. O'Brien, and P. Schiffer, *Phys. Rev. Lett.* **96**, 027216 (2006).
- <sup>26</sup>M. Blume, L. M. Corliss, J. M. Hastings, and E. Schiller, *Phys. Rev. Lett.* **32**, 544 (1974).
- <sup>27</sup>W. P. Wolf, *Braz. J. Phys.* **30**, 794 (2000).
- <sup>28</sup>T. Morinaga (unpublished).